Korean J Physiol Pharmacol 2022;26(3):145-155
https://doi.org/10.4196/kjpp.2022.26.3.145

KJPP

Original Article

Chemosensitizing effect and mechanism of imperatorin on the anti-tumor activity of doxorubicin in tumor cells and transplantation tumor model

Xin-li Liang[1], Miao-miao Ji[1], Zheng-gen Liao[1], Guo-wei Zhao[1], Xi-lan Tang[2], and Wei Dong[1,*]

[1]*Key Laboratory of Modern Preparation of Chinese Medicine, Ministry of Education, Jiangxi University of Chinese Medicine, Nanchang 330004,* [2]*Jiangxi Provincial Key Laboratory of Drug Design and Evaluation, School of Pharmacy, Nanchang 330013, China*

ARTICLE INFO

Received December 4, 2020
Revised November 7, 2021
Accepted February 2, 2022

***Correspondence**
Wei Dong
E-mail: Paln7@163.com

Key Words
Doxorubicin
Imperatorin
Leukemia
Multidrug resistance
P-glycoprotein

ABSTRACT Multidrug resistance of tumors has been a severe obstacle to the success of cancer chemotherapy. The study wants to investigate the reversal effects of imperatorin (IMP) on doxorubicin (DOX) resistance in K562/DOX leukemia cells, A2780/Taxol cells and in NOD/SCID mice, to explore the possible molecular mechanisms. K562/DOX and A2780/Taxol cells were treated with various concentrations of DOX and Taol with or without different concentrations of IMP, respectively. K562/DOX xenograft model was used to assess anti-tumor effect of IMP combined with DOX. MTT assay, Rhodamine 123 efflux assay, RT-PCR, and Western blot analysis were determined *in vivo* and *in vitro*. Results showed that IMP significantly enhanced the cytotoxicity of DOX and Taxol toward corresponding resistance cells. *In vivo* results illustrated both the tumor volume and tumor weight were significantly decreased after 2-week treatment with IMP combined with DOX compared to the DOX alone group. Western blotting and RT-PCR analyses indicated that IMP downregulated the expression of P-gp in K562/DOX xenograft tumors in NOD/SCID mice. We also evaluated glycolysis and glutamine metabolism in K562/DOX cells by measuring glucose consumption and lactate production. The results revealed that IMP could significantly reduce the glucose consumption and lactate production of K562/DOX cells. Furthermore, IMP could also remarkably repress the glutamine consumption, α-KG and ATP production of K562/DOX cells. Thus, IMP may sensitize K562/DOX cells to DOX and enhance the anti-tumor effect of DOX in K562/DOX xenograft tumors in NOD/SCID mice. IMP may be an adjuvant therapy to mitigate the multidrug resistance in leukemia chemotherapy.

INTRODUCTION

Malignant tumors have become one of the most important causes of human death. According to the World Health Organization's World Cancer Report 2014, cancer caused 8.2 million deaths worldwide in 2012, and this number is expected to rise to 22 million by 2035 [1]. Chemotherapy plays an important role in the integrated therapy of malignant tumors, and the combination of chemotherapy with operation and radiotherapy represents the three methods of treatment for malignant tumors [2]. However, the multidrug resistance (MDR) of tumors affects the efficacy of clinical chemotherapy and remains the main cause of chemo-

Author contributions: X.L.L. contributed in collecting materials,design of the experiment and analysis of the data and drafted the paper. X.L.L. and M.M.J. contributed the experiment and instigation work, M.M.J. contributed to do the cell experiments and revising the manuscript, Z.G.L. contributed in the animal experiment and running the part of laboratory work. G.W.Z. and W.D. contributed to chromatographic analysis and critical reading of the manuscript. X.L.T. contributed to the design of the experiments and W.D. contributed to the edition of the manuscript. All the authors have read the final manuscript and approved the submission.

therapy failure [3-6]. Many first-line drugs used to treat cancer, such as doxorubicin, taxanes, and vinblastine alkaloids can cause MDR [7-11]

The mechanism of MDR induction in cancers is complex, but high expression of P-glycoprotein (P-gp) is thought to be one of the main causes of MDR. Previous studies [12-15] have shown that P-gp is highly expressed in breast cancer, ovarian cancer, gastric cancer, leukemia, and other tumors. High expression of P-gp is associated with the emergence of MDR and a reduced response to chemotherapy in many cancers. P-gp can extrude drugs with diverse structures from cells using energy provided by ATP hydrolysis, decreasing the drug concentration in cells and subsequently reducing the efficacy of chemotherapeutic agents [16]. Therefore, inhibition of P-gp mediated drug efflux is thought to be an effective method to resensitize multidrug-resistant cancer cells to chemotherapy.

Researchers have found that many traditional Chinese medicines (TCMs), active compounds of TCMs and serum containing TCMs can reverse multidrug resistance of cancers, and are characterized by high efficiency, low toxicity, multiple targets, and strong specificity. Currently, screening P-gp reversal agents based on TCM has received increasingly attention [17,18]. It was previously reported that the active ingredients of TCM, such as daurisine, daurisoline [19], quercetin, genistein and so on [20,21], can inhibit the efflux of ATP-binding cassette transporters, including P-gp, multidrug resistance-associated protein, and breast cancer resistance protein. To study the effect of the active ingredients of TCM on the reversal of MDR may be of great significance for the development of chemosensitizers.

As shown in Fig. 1, Imperatorin (IMP) is a linear furocoumarin compound isolated from the root of *Angelica dahurica*, *Euphorbia chinensis*, *Cnidium mongolicum*, and *Angelica sinensis*. Modern pharmacological studies have shown that IMP is a major bioactive furanocoumarin [22], and it has long been known that IMP exhibits many biological activities, such as anti-tumor [23], anti-bacterial, anti-viral and anti-oxidant effects [24,25]. Reports have shown that IMP inhibits proliferation, promotes apoptosis and interferes with the signal transduction of cancer cells [26,27]. However, the effects of IMP on tumor-resistant cells have not been studied. In this study, we determined whether IMP can reverse the multidrug resistance of human leukemia cells to chemotherapeutic agents using *in vitro* and *in vivo* approaches.

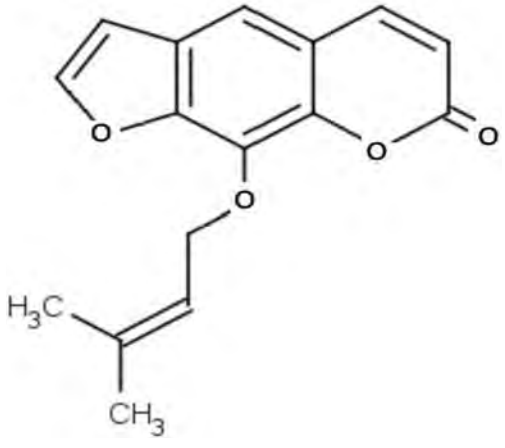

Fig. 1. The chemical structure of imperatorin (IMP).

METHODS

Chemicals, reagents and botanical material

IMP was purchased from the National Institutes for Food and Drug Control (Beijing, China) and its purity exceeds 99%. Epirubicin hydrochloride was obtained from Lunan Pharmaceutical (batch: 155160702). The Thermo Scientific RevertAid First cDNA Synthesis Kit was provided by Thermo Fisher Scientific. The Trizol RNA Extraction Kit was purchased from Ambion (Thermo Fisher Scientific, Beijing, China). The reverse transcription kit was purchased from Promega (Madison, WI, USA). Power SYBR Green PCR Mix was purchased from Life Technologies, Inc., (New York, NY, USA) PCR primers were synthesized by Shanghai Sangon Biotech Co. Ltd. (Shanghai, China). A mouse monoclonal anti-P-gp (MDR) antibody was obtained from Sigma-Aldrich, Inc. (St. Louis, MO, USA) A GAPDH mouse monoclonal antibody was purchased from Shanghai Bioleaf Biotech Co. Ltd. (Shanghai, China). Horseradish peroxidase (HRP)-conjugated goat anti-mouse immunoglobulin G (IgG), radio immunoprecipitation assay (RIPA) lysis buffer, protease inhibitors, phosphatase inhibitors, bicinchoninic acid (BCA) Protein Assay Reagent Kit, and enhanced chemiluminescence (ECL) Kit were purchased from Beijing Com Win Biotech Co. Ltd. (Beijing, China).

Cell culture

Human chronic myelogenous leukemia cell line K562 and its doxorubicin-resistant cell line K562/DOX, human ovary A2780 cell line and its Taxol-resistant cell line A2780/Taxol were all purchased from Shanghai Gefan Biotechnology. Co., Ltd. (Shanghai, China) Cells were grown in an atmosphere of 5% CO_2 at 37°C and cultured in RPMI 1640 medium containing 10% fetal bovine serum and 100 U/ml penicillin-streptomycin. Drug-resistant cell lines were maintained with suitable concentrations of drugs,, and the drugs were withdrawn 2 weeks before experiments.

Cytotoxicity assays

Cell viability and proliferation was determined by Cell Counting Kit-8 (CCK-8) assay. Different cells were seeded into 96-well plates and incubated overnight. Drug at concentrations in the presence or absence of IMP (2.78, 5.56, 11.10 μM) were added to corresponding cells, respectively. After incubation for 48 h, 20 μl

of the CCK-8 reagent was added to each well, and the absorbance was determined at 450 nm after 3 h. 50% inhibiting concentration (IC_{50}) was calculated from survival curves using the Bliss method. The resistance index (RI) was calculated by dividing the IC_{50} value of K562/DOX cells by that of K562 cells. The reversal fold (RF) was calculated as the ratio between the IC_{50} value alone to that of IMP combined with chemotherapeutic drugs.

Detection of Rhodamine 123 (Rho 123)

K562 and K562/DOX cells were plated in 12-well plates and then incubated different concentration of drugs or Hank's balanced salt solution (HBSS, 37°C, pH 7.4). Cells were incubated in a 5% CO_2 incubator at 37°C. The reaction was terminated after 60 min on ice. The solution was separated by centrifuging at 1,000 rpm for 5 min at 4°C, discarded the supernatant and washed for twice with cold HBSS. Rho 123 (5 μM) was added in different groups and incubated for 75 min. The accumulation was stopped by rinsing cells with ice-cold HBSS. Single-cell suspensions were prepared and centrifuged at 12,000 *g* for 10 min, and the protein concentrations were determined using BCA protein assay kit. The concentration of Rho 123 in each tube was divided by the total protein content of each tube to eliminate errors caused by the number of cells. In a parallel experiment, 200 μl of supernatant was mixed with 300 μl of acetonitrile followed by centrifugation at 14,000 *g* for 20 min. Rho 123 in the supernatant was detected by a previously established high-performance liquid chromatography (HPLC) method. Chromatographic separation was achieved on a Phenomenex-C18 (250 mm × 4.6 mm, 5 μm) column with acetonitrile/1% triethylamine (pH 3.0) under gradient conditions at a flow rate of 1 ml/min. Detection was performed using a fluorescence detector with an excitation wavelength of 485 nm and an emission wavelength of 546 nm [28].

K562/DOX xenograft NOD/SCID mice model

Male SPF NOD/SCID mice (20 ± 2 g) were provided by the Nanjing Institute of Biomedicine of Nanjing University (Laboratory animal certificate number, 201901A014). Animals were housed under standard conditions of artificial light and dark cycles with free access to food and water, and the room had good ventilation with a temperature at 20°C–25°C. All animal studies were performed according to the approved protocols and guidelines of the Institutional Animal Ethical Care Committee.

K562/DOX cells (1×10^7 cells/0.2 ml) were subcutaneously injected into the right flanks of 10 NOD/DSCID mice. When the tumor nodules were approximately 1 cm in diameter, they were subcultured to establish a transplanted tumor model. The model mice were randomly divided into the following 5 groups: model group (intraperitoneal injection of 0.9% saline once daily), DOX alone group (intraperitoneal injection of DOX at a dose of 2.5 mg/kg, twice a week), low-dose IMP combined with DOX group (oral administration of IMP at a dose of 5 mg/kg once daily, and intraperitoneal injection of DOX at a dose of 2.5 mg/kg, twice a week), medium-dose IMP combined with DOX group (oral administration of IMP at a dose of 10 mg/kg once daily, and intraperitoneal injection of DOX at a dose of 2.5 mg/kg, twice a week), and high-dose IMP combined with DOX group (oral administration of IMP at a dose of 20 mg/kg once daily, and intraperitoneal injection of DOX at a dose of 2.5 mg/kg, twice a week). Mice were continuously treated for 15 days, and tumor volumes were measured once a week. Animals were sacrificed, and the tumor tissues were removed and weighed after the last treatment.

Histopathology

Tumor tissues were immobilized in 4% formaldehyde solution, embedded in paraffin, sectioned and stained with hematoxylin and eosin (H&E).

Transmission electron microscopy

Tumor tissues were immobilized in 2.5% glutaraldehyde, dehydrated, embedded, cut into 80 nm sections, and stained with 2% uranium acetate and citrate. A JEM-1011 transmission electron microscope was used to observe the tumor ultrastructural changes.

ELISA analysis

Cell glycolysis, glutamine consumption, α-ketoglutaric acid (α-KG) production and ATP production were assessed by Glucose Assay Kit, Lactate Assay Kit, the Glutamine Assay Kit, α-KG Assay Kit and ATP Assay Kit according to the manufacturer's instructions.

Detection of cell extracellular acidification rate

Cell extracellular acidification rate were performed to determine cellular aerobic glycolysis. In brief, 5×10^4 Cells were seeded into the cell-culture dish overnight (96-well microplate), and in the 20 min added 10 mM of Glucose, 1 μM of Oligomycin add in 15 min, and 50 mM of 2-deoxy-D-glucose (2-DG) put in it another 15 min. Finally we used Glycolysis Rate Determination Kit to test, and then analyzed by Seahorse XFe Extracellular Flux Analyzer (Seahorse Bioscience, North Billerica, MA, USA).

Western blot analysis

Tumor tissues were lysed in RIPA buffer containing phenylmethanesulfonyl fluoride and phosphatase inhibitor. The concentration of total protein was detected by an Enhanced BCA Protein Assay Kit. Equal quantities of protein were separated by sodium dodecyl sulfate polyacrylamide gel electrophoresis and then transferred to PVDF membrane. Membranes were blocked

in 5% bovine serum albumin) for 1 h and incubated with primary antibodies overnight. Membranes were then incubated with secondary antibodies at room temperature for 1 h. Proteins were detected by using an ECL Western blotting detection system.

Real-time polymerase chain reaction (RT-PCR)

The total RNA of tumor tissues was extracted by the RNA easy Total RNA mini kit and reverse transcribed to cDNA with reverse transcription kit according to the manufacturer's protocol, respectively. PCR primer design and synthesis were performed by the primer design software provided by Applied Biosystems. The primer sequences were as follows: human *MDR1*, forward 5′-AAA GCG ACT GAA TGT TCA GTG G-3′, reverse 5′-TGC GTG TGG AGT ATT TGG ATG-3′; human *hRpIP1v-F* (internal control), forward 5′-CCC TCA TTC TGC ACG ACG AT-3′, reverse 5′-GGC TCA ACA TTT ACA CCG GC-3′. PCR amplification was performed using Power SYBR Green PCR Mix according to the manufacturer's protocol.

Statistical analysis

All experiments were carried out at least three times. SPSS software (SPSS Inc., Chicago, IL, USA) was used for statistical analysis. All of the data were expressed as mean ± SD, and were subjected to statistical analysis by one-way ANOVA followed by a Student–Newman–Keuls *post-hoc* test. $p < 0.05$ was considered significant for all tests.

RESULTS

Drug resistant testing of K562/DOX and A2780/Taxol cell lines

Both DOX and Taxol exhibited anti-proliferative activity on both parental and resistant cells dose-dependently (Fig. 2A, C), respectively. The IC_{50} values of K562 was 1.63 ± 0.20 μM, whereas IC_{50} values of K562/DOX was 38.20 ± 0.58 μM. The RI for K562/DOX cells was 23.43 (Fig. 2B, Table 1) (RI > 15). The IC_{50} values of A2780 was 51.33 ± 1.76 μM, whereas IC_{50} values of A2780/Taxol was 188.30 ± 4.63 μM.The RI for A2780/Taxol cells was 3.67 (Fig. 2D, Table 2). The results showed that the two kinds of resistant cell lines were all strongly resistant to corresponding chemotherapy drugs and can be used for follow-up research.

Reversal effect of IMP on drug resistance cell lines of K562/DOX and A2780/Taxol

Treatments with IMP at concentrations of 2.78, 5.56, and 11.10 μM significantly increased the cytotoxicity of DOX in K562/DOX cells ($p < 0.05$), respectively, but had little effect in K562 cells (Fig. 3A, B and Table 1). IMP showed a dose-dependent reversal effect of drug resistance of K562/DOX cells. Treatments with IMP at concentrations of 7.40, 18.50, and 37.00 μM significantly increased the cytotoxicity of Taxol in A2780/Taxol cells ($p < 0.05$), respectively, while had little effect in A2780 cells (Fig. 3C, D and Table 2). IMP showed a dose-dependent reversal effect of drug resistance of A2780/Taxol cells. As shown in Table 1, as the concentration of IMP increased, the IC_{50} value of DOX-IMP

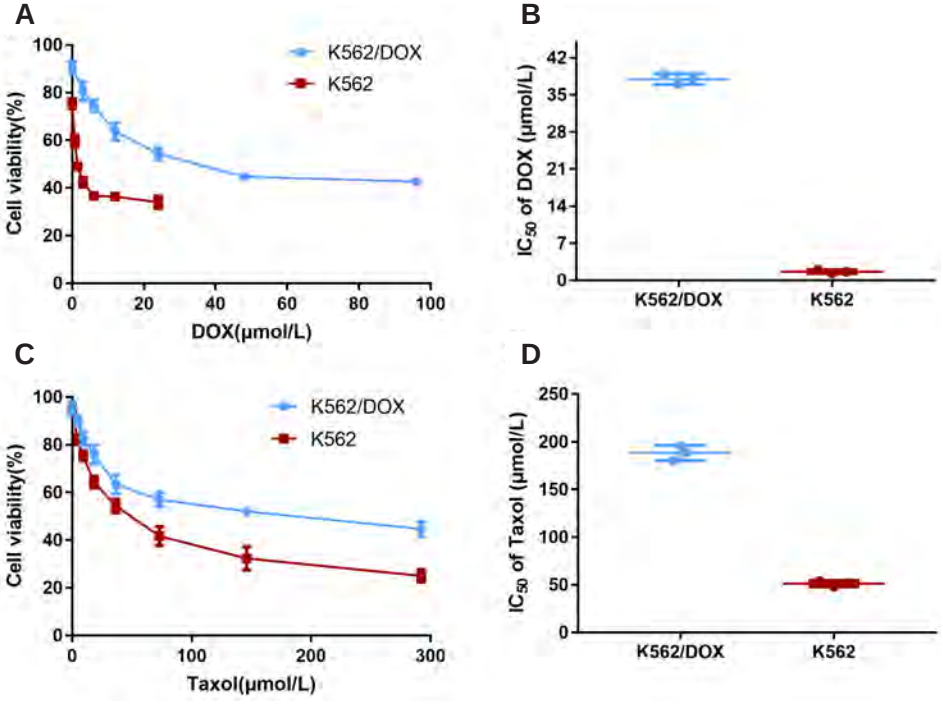

Fig. 2. The resistance index of resistant cell line of K562/DOX and A2780/Taxol. (A) Cell survival rate of different concentration of DOX on K562 and K562/DOX. (B) IC_{50} (μmol/L) values were calculated from survival curves using the Bliss method and then RI was calculated by dividing the IC_{50} for K562/DOX cells by that of K562 cells. (C) Cell survival rate of different concentration of Taxol on A2780 and A2780/Taxol. (D) IC_{50} (μM) values were calculated from survival curves using the Bliss method and then RI was calculated by dividing the IC_{50} for A2780/DOX cells by that of A2780 cells. Taxol, Taxinol; DOX, doxorubicin; IC_{50}, 50% inhibiting concentration; RI, resistance index.

Table 1. IC_{50} value in K562 cells and K562/DOX cells

Group	IC_{50} (μM)		RI	RF
	K562	K562/DOX		
DOX	1.63 ± 0.20	38.2 ± 0.58*	23.43	-
DOX + IMP (2.78 μM)	2.06 ± 0.18	9.38 ± 0.07*,†	4.55	5.15
DOX + IMP (5.56 μM)	1.93 ± 0.09	4.56 ± 0.13*,†	2.36	9.93
DOX + IMP (11.10 μM)	2.08 ± 0.19	3.50 ± 0.07*,†	1.68	13.95

Data are shown as means ± SD, n = 3. K562 and K562/DOX cells were incubated with various concentrations of DOX (0.36–92.00 μM) in the presence or absence of IMP (2.78, 5.56, 11.10 μM) for 48 h, respectively. The cytotoxicity was evaluated by CCK-8 assay. IC_{50} (μM) values were calculated using the Bliss method. RI was calculated by dividing the IC_{50} for K562/DOX cells by that of K562 cells. RF was calculated as the ratio between the IC_{50} value of DOX alone to that of IMP combined with DOX in K562/DOX cells. IC_{50}, 50% inhibiting concentration; RI, resistance index; RF, reversal fold; DOX, doxorubicin; IMP, imperatorin; CCK-8, Cell Counting Kit-8. *$p < 0.05$ *vs*. respective K562 cells; †$p < 0.05$ *vs*. respective DOX alone group.

Table 2. IC_{50} value in A2780 cells and A2780/Taxol cells

Group	IC_{50} (μM)		RI	RF
	A2780	A2780/Taxol		
Taxol	51.33 ± 1.76	188.30 ± 4.63*	3.67	-
Taxol + IMP (7.40 μM)	52.84 ± 1.18	83.29 ± 2.21*,†	1.58	2.32
Taxol + IMP (18.50 μM)	56.89 ± 2.01	71.05 ± 2.13*,†	1.25	2.94
Taxol + IMP (37.00 μM)	51.57 ± 2.11	35.53 ± 1.17*,†	0.69	5.32

Data are shown as means ± SD, n = 3. A2780 and A2780/Taxol cells were incubated with various concentrations of Taxol (0.76–97.12 μM) in the presence or absence of IMP (7.40, 18.50, 37.00 μM) for 48 h, respectively. The cytotoxicity was evaluated by CCK-8 assay. IC_{50} (μM) values were calculated using the Bliss method. RI was calculated by dividing the IC_{50} for A2780/Taxol cells by that of A2780 cells. RF was calculated as the ratio between the IC_{50} value of Taxol alone to that of IMP combined with Taxol in A2780/Taxol cells. IC_{50}, 50% inhibiting concentration; Taxol, Taxinol; RI, resistance index; RF, reversal fold; IMP, imperatorin; CCK-8, Cell Counting Kit-8. *$p < 0.05$ *vs*. respective A2780 cells; †$p < 0.05$ *vs*. respective Taxol alone group.

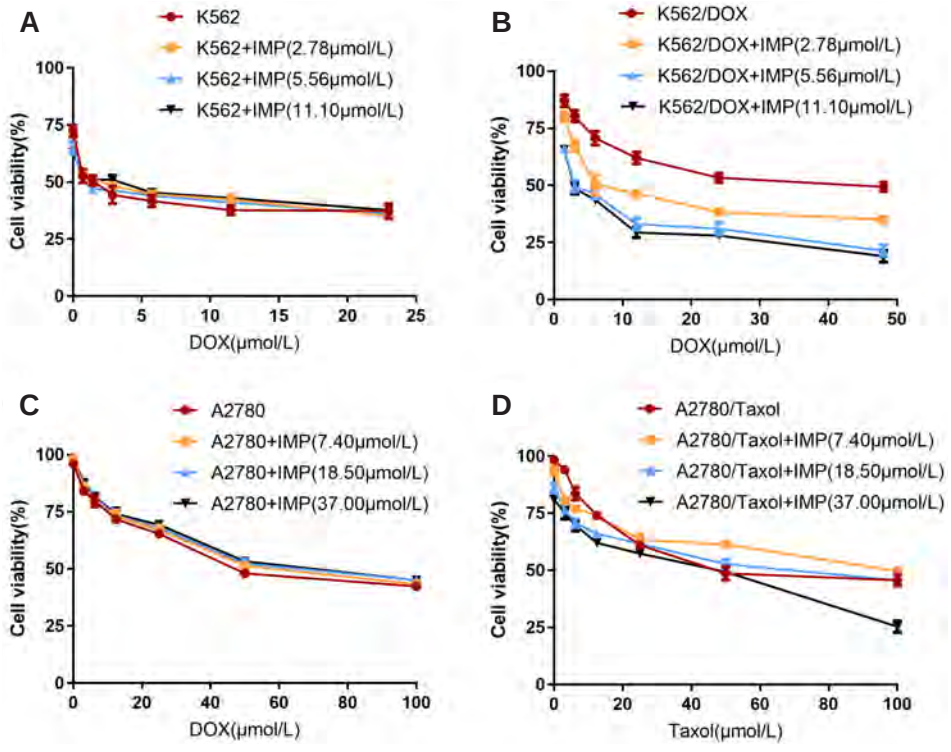

Fig. 3. Chemosensitizing effect analysis of IMP on various tumor-resistant cell lines. (A) Cell viability of different concentrations of DOX combined with IMP (2.78, 5.56, and 11.10 μM) on K562 cells. (B) Cell viability of different concentrations of DOX combined with IMP (2.78, 5.56, and 11.10 μM) on K562/DOX cells. (C) Cell viability of different concentrations of Taxol combined with IMP (7.40, 18.50, and 37.00 μM) on A2780 cells. (D) Cell viability of different concentrations of Taxol combined with IMP (7.40, 18.50, and 37.00 μM) on A2780/Taxol cells. Representative data from three independent experiments. IMP, imperatorin; DOX, doxorubicin; Taxol, Taxinol.

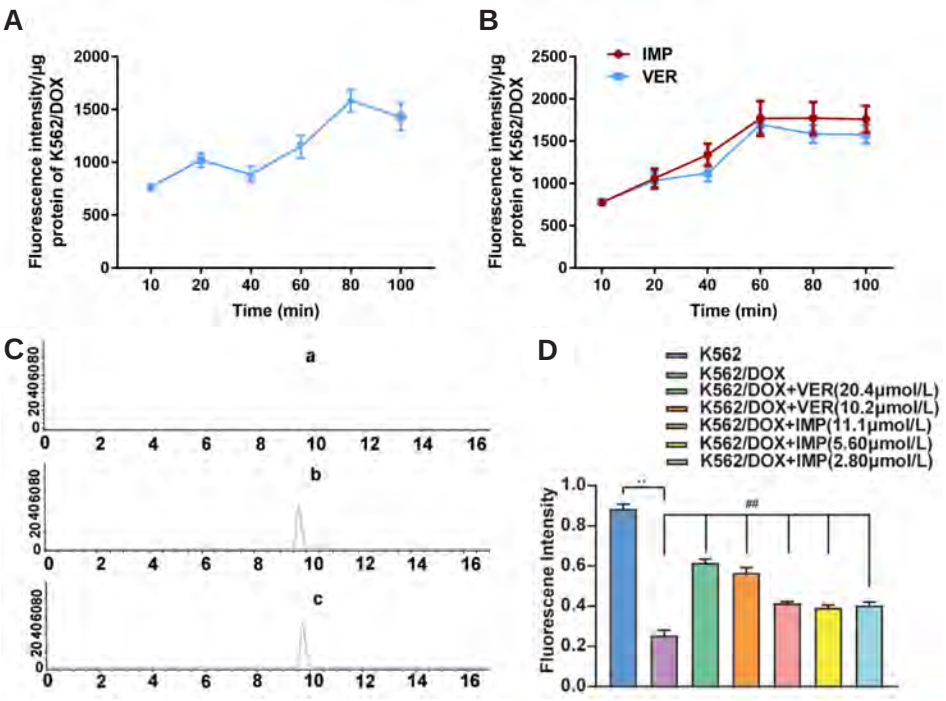

Fig. 4. Effect of IMP on intracellular accumulation of Rho 123. (A) Effect of time on the fluorescence intensity of Rho 123 in K562/DOX cells. (B) Effect of the coincubation time of Rho 123 and drugs on the fluorescence intensity of Rho 123 in K562/DOX cells. (C) HPLC method specificity. (C-a) K562/DOX cells solution. (C-b) K562/DOX cells solution containing Rho 123 reference solution. (C-c) K562/DOX cells solution after incubation with Rho 123 for 75 min. (D) Effect of IMP on intracellular accumulation of Rho 123 in K562 cells and K562/DOX cells. K562/DOX cells treated with 10.2 and 20.4 μmol/L VER, which used as the positive control. Data are shown as means ± SD, n = 3. IMP, imperatorin; DOX, doxorubicin; Taxol, Taxinol; HPLC, high-performance liquid chromatography; VER, verapamil. **p < 0.01 *vs.* K562 cells. ##p < 0.01 *vs.* K562/DOX cells untreated group.

combinations reduced and resulting in the increased RF of IMP accordingly (RF from 3.33 to 9.00). We also can see in Table 2, with the concentration of IMP increased,the IC_{50} value of Taxol-IMP combinations reduced and resulting in the increased RF of IMP accordingly (RF from 2.75 to 6.29). These results indicated that IMP could sensitiz the different tumor-resistant cell lines to chemotherapeutics.

Effect of IMP on intracellular accumulation of Rho 123

Rho 123, a fat-soluble fluorescent substance and a substrate of P-gp, which can be transported from the cell membrane into the cytoplasm. While P-gp can discharge entered Rho 123 out of the cells. Therefore, the less amount of intracellular accumulation of Rho 123, the higher activity of P-gp. Verapamil is a P-gp inhibitor which could increase the amount of intracellular accumulation of Rho 123 [15]. We first examined the uptake of Rho 123 by K562/DOX cells. The results showed that the fluorescence intensity in K562/DOX cells increased with time, and gradually reached saturation state after a certain time (Fig. 4A). Therefore, 75 min was choosen as the coincubation time of Rho 123 and the impacts of IMP on the accumulation of Rho 123 in K562 cells and K562/DOX cells was observed. We further confirmed the effect of time on the absorption of IMP and verapamil (VER). The results showed that the fluorescence intensity of IMP increased with time just like VER, and gradually reached saturation state at 60 min (Fig. 4B). The HPLC detection showed that K562/DOX cell solution had no interference with the determination of Rho 123 (Fig. 4C). Next, we used HPLC detection method to observe the effects of IMP and VER on the accumulation of Rho 123 in K562 cells and K562/DOX cells. As shown in Fig. 4D, compared with K562 cells, there was a decreased accumulation and increased efflux of Rho 123 in K562/DOX cells, which is transported by P-gp ($p < 0.05$). IMP at concentrations of 2.78, 5.56, and 11.10 μmol/L significantly increased the intracellular Rho123 accumulation in K562/DOX cells ($p < 0.01$), implying that IMP may reduce the efflux activity of P-gp. The reference group VER at concentrations of 10.2, and 20.4 μM illustrated the same effect but more potently ($p < 0.01$).

IMP inhibiting restraining the glycolysis and glutamine metabolism of K526/DOX cells *in vitro*

Glycolysis and glutamine metabolism are important energy sources of cancer cells, and are also an important way for P-gp to inhibit drug efflux. We found that the expressin of P-gp was significantly increased in K562/DOX cells (Fig. 5A). We evaluated glycolysis and glutamine metabolism in K562/DOX cells by measuring glucose consumption and lactate production. The results revealed that IMP could significantly reduce the glucose consumption and lactate production of K562/DOX cells (Fig. 5B, C). Furthermore, IMP could also remarkably repress the glutamine consumption, α-KG production and ATP production of K562/DOX cells (Fig. 5D, E).

Effect of IMP combined with DOX on tumor growth of K562/DOX xenograft tumors in NOD/SCID mice

The tumor volume was measured every 7 days. Fig. 6A showed that both DOX alone and IMP combined with DOX treatments

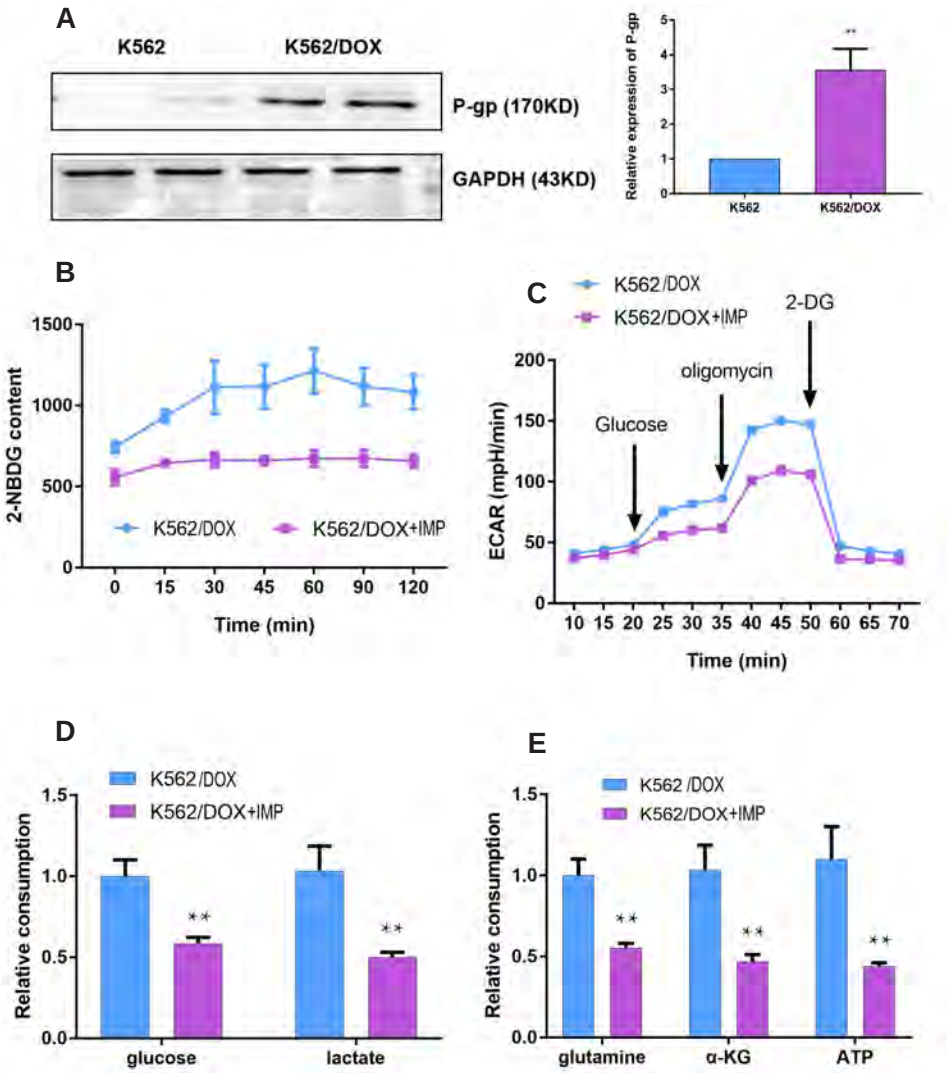

Fig. 5. IMP restrained the glycolysis and glutamine metabolism of K526/DOX cells *in vitro*. (A) DOX promoted the expression of P-gp. (B, C) The glucose consumption, lactate production and ECAR were measured to assess cell glycolysis. (D, E) Glutamine consumption, α-KG production and ATP production were determined using corresponding Assay Kits, respectively. K562/DOX cells treated with 0 and 2.8 μM IMP. IMP, imperatorin; DOX, doxorubicin; P-gp, P-glycoprotein; ECAR, extracellular acidification rate; α-KG, α-ketoglutaric acid; 2-DG, 2-deoxy-D-glucose. **p < 0.01.

significantly reduced the average tumor volume at 14 days, but not obvious at 0 day and 7 days. IMP combined with DOX treatments tended to reduce the average tumor volume at 14 days, as compared with the DOX alone treatment. After 14 days, mice were sacrificed and the tumor tissues were weighed. Compared with the untreated model group, both DOX alone and IMP combined with DOX treatments significantly decreased the tumor weight. Moreover, the average tumor weight in groups of IMP at dosage of 10 mg/kg and 20 mg/kg combined with DOX was remarkably lower than that in DOX alone group, respectively (Fig. 6B, 6C).

H&E staining showed increased necrosis and apoptosis in tumor tissues collected from mice treated with DOX alone and IMP combined with DOX (Fig. 7A). IMP (10 mg/kg and 20 mg/kg) combined with DOX group showed increased necrosis compared to the other groups, and fibrous tissue hyperplasia was found between tumors in IMP (20 mg/kg) combined with DOX group. The blue arrow indicates that the cell structure was seriously damaged and the cell density was enhanced.

Dual staining with 2% uranium acetate and lead citrate were visualized with transmission electron microscopy. The red arrows indicated mitochondria, we could see the swelling or rupture of mitochondria. And the green arrows indicated normol cell structure, it showed that Mitochondria were uniform in size and clear in structure. As illustrated in Fig. 7B, obvious necrosis, cytoplasmic vacuole, and apoptotic characteristics appeared in some cells of both DOX alone and IMP (10 mg/kg and 20 mg/kg) combined with DOX groups, respectively.

Effect of IMP combined with DOX on P-gp protein and mRNA expressions *in vivo*

We next examined whether IMP affected P-gp protein and mRNA expressions in K562/DOX xenograft tumor tissues in NOD/SCID mice through western blotting and quantitative RT-PCR experiments, respectively. As shown in Fig. 8, compared with the untreated model group, both DOX alone and IMP combined with DOX treatments significantly inhibited P-gp protein

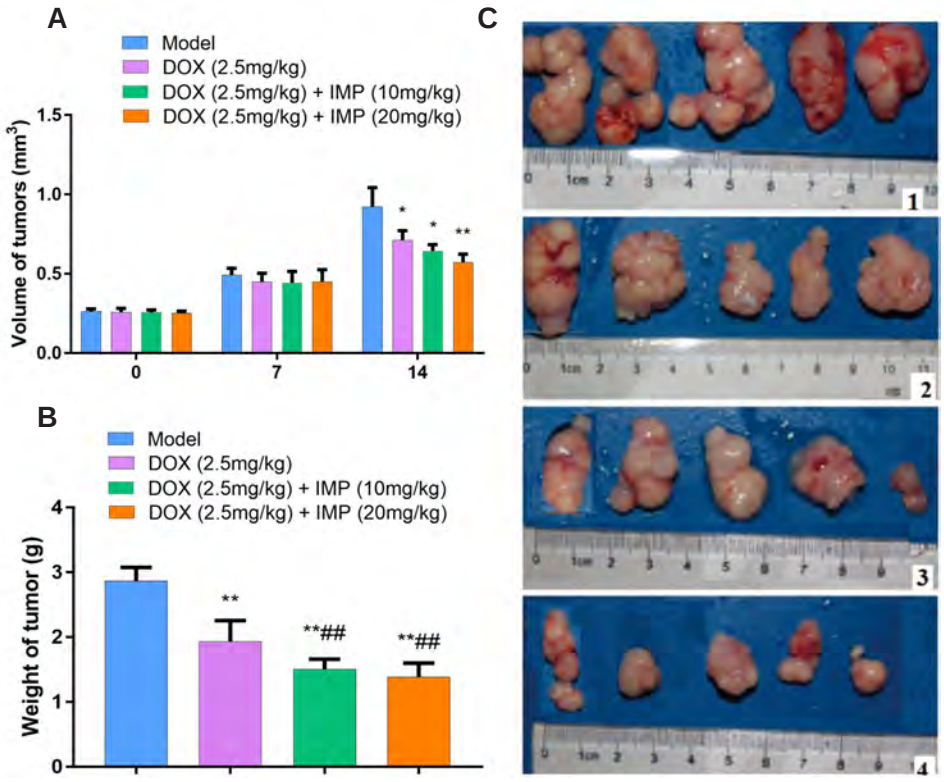

Fig. 6. Effect of IMP combined with DOX on tumor growth of K562/DOX xenograft tumors in NOD/SCID mice. (A) The tumor volumes were measured at 0, 7, and 14 days. (B) The tumor weights were analyzed after 14 days. (C) Representative images of tumor tissues subjected to different treatments of DOX and IMP (1, untreated model group; 2, DOX 2.5 mg/kg alone group; 3, IMP 10 mg/kg + DOX 2.5 mg/kg group; 4, IMP 20 mg/kg + DOX 2.5 mg/kg group). Data are shown as means ± SD, n = 8. IMP, imperatorin; DOX, doxorubicin. *$p < 0.05$; **$p < 0.01$ *vs.* untreated model group. ##$p < 0.01$ *vs.* DOX 2.5 mg/kg alone group.

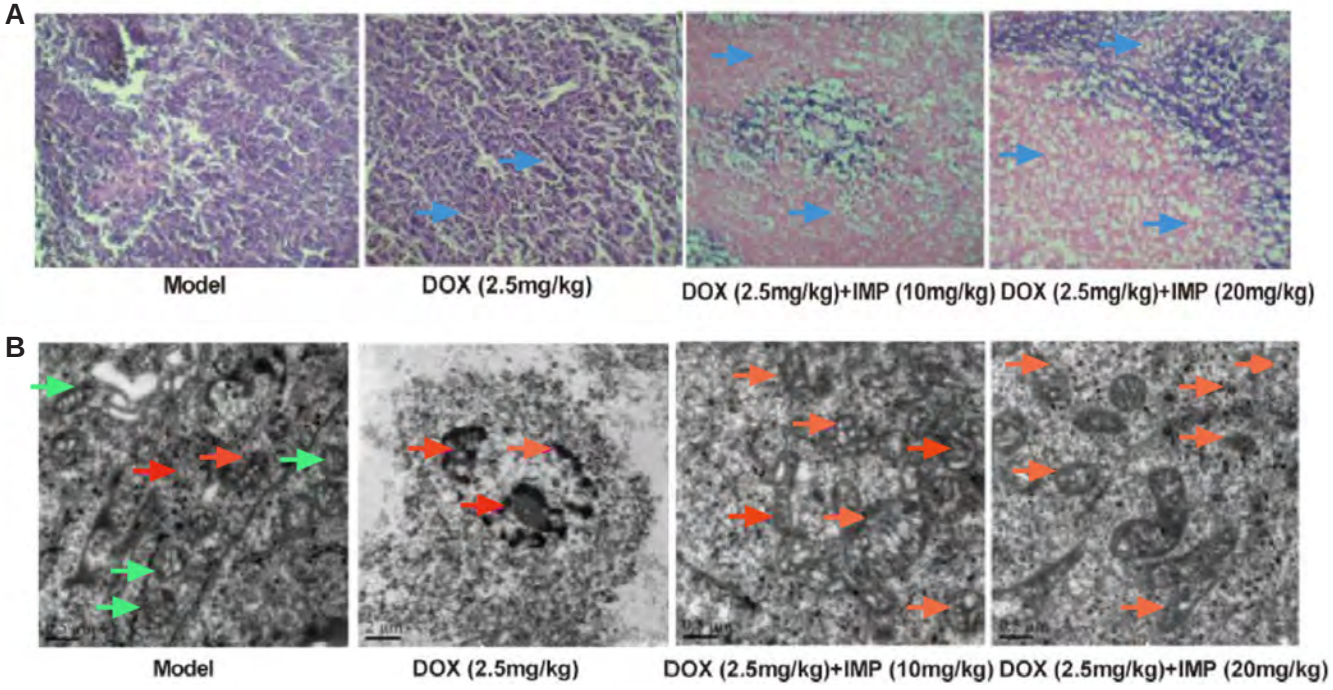

Fig. 7. Effect of IMP combined with DOX on pathological abnormalities of K562/DOX xenograft tumors in NOD/SCID mice. (A) Tumor tissues were fixed, sectioned, and stained with H&E (magnification, ×50). The blue arrows indicate that the cell structure was seriously damaged and the cell density was enhanced. (B) Electron microscope observation of tumor tissues subjected to different treatments with IMP (10 and 20 mg/kg) and DOX (2.5 mg/kg). The red arrows indicated mitochondria indicates that the cells have shrinkage, necrosis, cytoplasmic vacuoles. The orange arrows were more obvious mitochondrial structure. The green arrows pointed out the mitochondrial morphology of normal cells. IMP, imperatorin; DOX, doxorubicin.

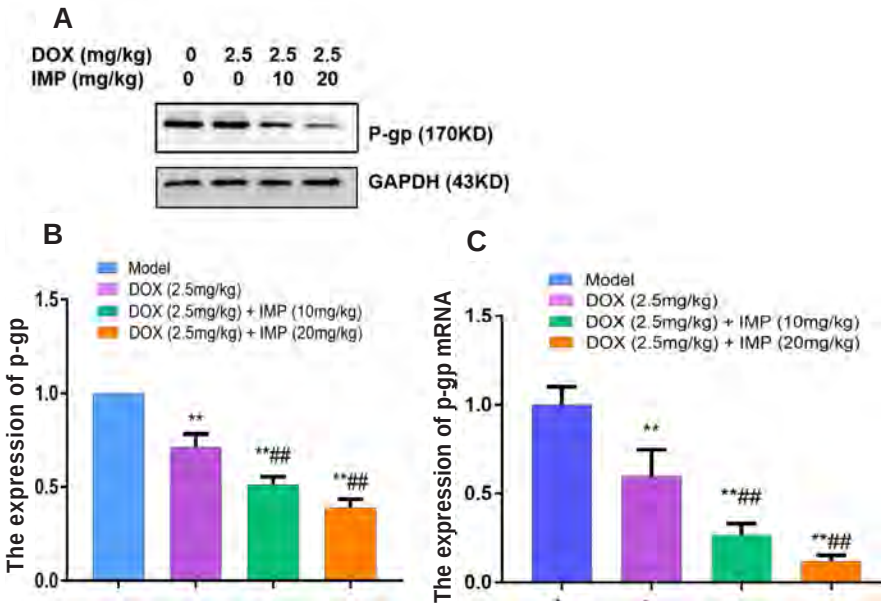

Fig. 8. Effect of IMP combined with DOX on P-gp expression in K562/DOX xenograft tumors in NOD/SCID mice. (A) Representative Western blots of P-gp protein. Quantified data showing IMP at dosage of 10 mg/kg and 20 mg/kg combined with DOX (2.5 mg/kg) treatments inhibited P-gp protein expression (B) and mRNA level (C) in K562/DOX xenograft tumor tissues as compared with DOX (2.5 mg/kg) alone treatment. Data are presented as the means ± SD, n = 8. IMP, imperatorin; DOX, doxorubicin; P-gp, P-glycoprotein. **p < 0.01 *vs.* untreated model group. ##p < 0.01 *vs.* DOX (2.5 mg/kg) alone group.

expression levels (Fig. 8A, B) and downregulated P-gp mRNA levels (p < 0.01, Fig. 8C). Moreover, IMP at dosage of 10 mg/kg and 20 mg/kg combined with DOX treatments further suppressed P-gp protein levels (Fig. 8A, B) and mRNA levels (Fig. 8C), as compared with the DOX alone treatment (p < 0.01), respectively. Our results indicated that IMP inhibited P-gp protein and mRNA expressions in K562/DOX xenograft tumor tissues in NOD/SCID mice.

DISCUSSION

MDR is one of the major problems in leukemia therapy. Thus, it is necessary to reverse the MDR of leukemia and improve the prognosis and survival rate of patients. Verapamil, one of the earliest reversal agents, it can reverse MDR via competitively combining with P-gp, and thus increasing the accumulation of intracellular chemotherapy drugs, but its use is limited by serious side effects. In recent years, natural medicine and Chinese herbal medicines have shown great advantages in reversing MDR. It has been reported that some extracts of traditional medicine, such as peoniflorin, curcumin, dauricine, quercetin, and procyanidin, effectively inhibit NF-κB activity, downregulate ABCB1 expression and decrease P-gp expression [29-35]. Previous studies have shown that IMP increases the intestinal absorption of anti-tumor agents (such as vincristine) [36] and improves the ATPase activity of P-gp [37]. Therefore, we think it might have the function of reversing the multidrug resistance whic associated with P-gp.

In this study, different tumor-resistant cell lines were used to confirm the chemosensitizing effect of IMP to chemotherapeutics. Results showed that IMP combined with chemotherapeutics treatments decreased RI value, as illustrated in Tables 1 and 2. Overexpression of P-gp is one of the most important causes of MDR [38]. Rhodamine-123 (6-amino-9-[2-293 methoxycarbonylphenyl) xanthen-3-ylidene] azanium chloride), a model substrate of P-gp, is a lipophilic, cationic fluorescent dye that has been used as a selective marker for studying the functional activity of P-gp [39]. Our results indicated that IMP increased the intracellular accumulation of Rho 123 in K562/DOX cells, which suggested that IMP could inhibit P-gp efflux activity in tumor-resistanct cells.

In order to further determine the mechanism of IMP inhibiting P-gp expression and regulating cell resistance, we detected the expression of P-gp in K562 cells and K562/DOX cells, and the effect of P-gp on DOX resistance was confirmed again. Previous studies have shown that IMP could enhance cell resistance to DOX and inhibit the efflux activity of P-gp. The efflux function of P-gp requires ATP, glycolysis and glutamine metabolism play an important role in it [40], a new study have found that the efflux of P-gp in DOX induced drug-resistant hepatocytes depends on mitochondrial ATP driven by glutamine, recently [41]. In this study, we also verified that glycolysis and glutamine metabolism was involved in the mechanism of IMP enhancing drug resistance. Combined with TEM observation of tumor tissue sections confirmed that IMP promoted the swelling or disappearance of mitochondria. Does it mean that IMP could inhibit mitochondrial activity, reduce ATP production, block glycolysis and gluta-

mine metabolism, and inhibit P-gp expression and reduce DOX efflux, so as to achieve drug resistance. These data indicated that P-gp might be an important mechanism of drug resistance, and IMP could inhibit the expression of P-gp by regulating glycolysis and glutamine metabolism. suggesting that IMP might be an important therapeutic option for drug resistance of tumor cells.

To verify the reversal of MDR by IMP in leukemia therapy, we used NOD/SCID mice to generate the K562/DOX xenograft leukemia model. In this model, the incidence of tumors is high, which is consistent with a previous report [42]. *In vivo* results indicated that both DOX alone and IMP combined with DOX treatments significantly reduced the average tumor volume and the average tumor weight, IMP combined with DOX treatments were able to remarkably lower the average tumor weight than that of DOX alone treatment. Interestingly, according to the pathological results, combination therapy of IMP and DOX showed more necrosis as well as fibrous tissue hyperplasia between tumors than that of DOX alone treatment. The efflux function of P-gp is related to protein and gene expression, so we further investigated the effect of IMP P-gp protein and gene expression *in vivo*. Our results indicated that compared with the DOX alone treatment, combination therapy of IMP and DOX could remarkably inhibit the protein and mRNA expressions of P-gp. IMP reversed MDR in K562/DOX cells may be related to the suppression of P-gp protein and gene expressions.

In summary, we evidenced that IMP was able to enhance the efficacy of conventional chemotherapeutic drug DOX in K562/DOX cells and K562/DOX xenograft NOD/SCID mice by inhibition of efflux function of P-gp and suppression of P-gp protein and gene expressions. These findings indicated that IMP may be a reversal agent for the treatment of leukemia, which may reduce the occurrence of MDR in leukemia chemotherapy and improve the efficiency of leukemia chemotherapy.

FUNDING

This study was supported by the Project of Education Department of Jiangxi Province (180639), Natural Science Foundation of Jiangxi Province (2018BAB215041), Foundation of Education Bureau of Jiangxi Province (GJJ180606), Project of Jiangxi University of TCM (JXSYLXK-ZHYAO081), and Open Project of Key Laboratory of Modern Preparation of TCM, Ministry of Education, Jiangxi University of Traditional Chinese MedicineChinese Medicine (TCM-201911).

ACKNOWLEDGEMENTS

We are grateful to Nanjing University of Traditional Chinese MedicineChinese Medicine for the supporting the model of K562/DOX Xenograft Tumors in NOD/SCID Mice. We thank Danny Wilson of the university of Adelaide for the suggestions in writing the paper.

CONFLICTS OF INTEREST

The authors declare no conflicts of interest.

REFERENCES

1. Abad MJ, de las Heras B, Silván AM, Pascual R, Bermejo P, Rodriquez B, Villar AM. Effects of furocoumarins from Cachrys trifida on some macrophage functions. *J Pharm Pharmacol.* 2001;53:1163-1168.
2. Al-Ali AAA, Nielsen RB, Steffansen B, Holm R, Nielsen CU. Non-ionic surfactants modulate the transport activity of ATP-binding cassette (ABC) transporters and solute carriers (SLC): relevance to oral drug absorption. *Int J Pharm.* 2019;566:410-433.
3. Al-Mohizea AM, Al-Jenoobi FI, Alam MA. Rhodamine-123: a p-glycoprotein marker complex with sodium lauryl sulfate. *Pak J Pharm Sci.* 2015;28:617-622.
4. Baek NI, Ahn EM, Kim HY, Park YD. Furanocoumarins from the root of Angelica dahurica. *Arch Pharm Res.* 2000;23:467-470.
5. Breier A, Barancík M, Sulová Z, Uhrík B. P-glycoprotein--implications of metabolism of neoplastic cells and cancer therapy. *Curr Cancer Drug Targets.* 2005;5:457-468.
6. Dong W, Guan X, Liao Z, Lu X, Liang X, Zhu W. [In vitro study on affinity of coumarins in Angelicae Dahuricae Radix and P-gp]. *Chin Tradit Herb Drugs*. 2016,47:2893-2896. Chinese.
7. Duran GE, Wang YC, Moisan F, Francisco EB, Sikic BI. Decreased levels of baseline and drug-induced tubulin polymerisation are hallmarks of resistance to taxanes in ovarian cancer cells and are associated with epithelial-to-mesenchymal transition. *Br J Cancer.* 2017;116:1318-1328.
8. Fan L, Jin B, Zhang S, Song C, Li Q. Stimuli-free programmable drug release for combination chemo-therapy. *Nanoscale.* 2016;8:12553-12559.
9. Fang S, Zhu W, Zhang Y, Shu Y, Liu P. Paeoniflorin modulates multidrug resistance of a human gastric cancer cell line via the inhibition of NF-κB activation. *Mol Med Rep.* 2012;5:351-356.
10. Ganta S, Amiji M. Coadministration of paclitaxel and curcumin in nanoemulsion formulations to overcome multidrug resistance in tumor cells. *Mol Pharm.* 2009;6:928-939.
11. Ge C, Cao B, Feng D, Zhou F, Zhang J, Yang N, Feng S, Wang G, Aa J. The down-regulation of SLC7A11 enhances ROS induced P-gp over-expression and drug resistance in MCF-7 breast cancer cells. *Sci Rep*. 2017;7:3791.
12. Gou Q, Liu L, Wang C, Wu Q, Sun L, Yang X, Xie Y, Li P, Gong C. Polymeric nanoassemblies entrapping curcumin overcome multidrug resistance in ovarian cancer. *Colloids Surf B Biointerfaces.* 2015;126:26-34.
13. Gottesman MM, Ling V. The molecular basis of multidrug resistance in cancer: the early years of P-glycoprotein research. *FEBS Lett.* 2006;580:998-1009.
14. Guan X, Yu S, Liao Z, Zhu W, Zhao G, Luo Y, Liang X. [Effects of 10

furanocoumarins in Angelica dahurica on intestinal transport of vincristine]. *Chin Tradit Herb Drugs.* 2015,46:2117-2121. Chinese.
15. Hait WN, Yang JM. Clinical management of recurrent breast cancer: development of multidrug resistance (MDR) and strategies to circumvent it. *Semin Oncol.* 2005;32(6 Suppl 7):S16-S21.
16. He L, Liu GQ. Interaction of multidrug resistance reversal agents with P-glycoprotein ATPase activity on blood-brain barrier. *Acta Pharmacol Sin.* 2002;23:423-429.
17. Jia Y, Sun S, Gao X, Cui X. Expression levels of TUBB3, ERCC1 and P-gp in ovarian cancer tissues and adjacent normal tissues and their clinical significance. *J BUON.* 2018;23:1390-1395.
18. Kocibalova Z, Guzyova M, Imrichova D, Sulova Z, Breier A. Overexpression of the ABCB1 drug transporter in acute myeloid leukemia cells is associated with downregulation of latrophilin-1. *Gen Physiol Biophys.* 2018;37:353-357.
19. Kozioł E, Skalicka-Woźniak K. Imperatorin-pharmacological meaning and analytical clues: profound investigation. *Phytochem Rev.* 2016;15:627-649.
20. Li J, Qin F, Yang P. [Reversal of multidrug resistance in human K562/ADM cell line by dauricine]. *J Dalian Med Univ.* 2002;24:94-96. Chinese.
21. Liang X, Dong W, Zhang J, Zhao G, Luo Y, Liao Z. Quantitative method study on transport mechanism of puerarin, berberine hydrochloride and paeoniflorin. Paper presented at: International Conference on Biotechnology and Medical Science; 2016 Apr 16-17; Nanjing, China. p. 280-292.
22. Li Z, Tan S, Li S, Shen Q, Wang K. Cancer drug delivery in the nano era: an overview and perspectives (review). *Oncol Rep.* 2017;38:611-624.
23. Li Z, Tang T, Liang X, Zhu J. [Imperatorin reverses multidrug resistance of Huma Oophoroma Cancer Cell A2780/Taxol and its mechanism]. *Pharmacol Clin Chin Mater Med.* 2019;35:31-33. Chinese.
24. Li Z, Wang C, Tang T, Liang X, Zhu J. [Effect of imperatorin on the content of Rho 123 in the drug-resistant cell suspension of tumor by HPLC-FLD]. *Chin J Pharm Anal.* 2019;9:1567-1573. Chinese.
25. Ma X, Hu M, Wang H, Li J. Discovery of traditional Chinese medicine monomers and their synthetic intermediates, analogs or derivatives for battling P-gp-mediated multi-drug resistance. *Eur J Med Chem.* 2018;159:381-392.
26. Mao X, Si J, Huang Q, Sun X, Zhang Q, Shen Y, Tang J, Liu X, Sui M. Self-assembling doxorubicin prodrug forming nanoparticles and effectively reversing drug resistance in vitro and in vivo. *Adv Healthc Mater.* 2016;5:2517-2527.
27. Mi C, Ma J, Wang KS, Zuo HX, Wang Z, Li MY, Piao LX, Xu GH, Li X, Quan ZS, Jin X. Imperatorin suppresses proliferation and angiogenesis of human colon cancer cell by targeting HIF-1α via the mTOR/p70S6K/4E-BP1 and MAPK pathways. *J Ethnopharmacol.* 2017;203:27-38.
28. Rigalli JP, Ciriaci N, Arias A, Ceballos MP, Villanueva SS, Luquita MG, Mottino AD, Ghanem CI, Catania VA, Ruiz ML. Regulation of multidrug resistance proteins by genistein in a hepatocarcinoma cell line: impact on sorafenib cytotoxicity. *PLoS One.* 2015;10:e0119502.
29. Sancho R, Márquez N, Gómez-Gonzalo M, Calzado MA, Bettoni G, Coiras MT, Alcamí J, López-Cabrera M, Appendino G, Muñoz E. Imperatorin inhibits HIV-1 replication through an Sp1-dependent pathway. *J Biol Chem.* 2004;279:37349-37359.
30. Shylasree TS, Bryant A, Athavale R. Chemotherapy and/or radiotherapy in combination with surgery for ovarian carcinosarcoma. *Cochrane Database Syst Rev.* 2013;2013:CD006246.
31. Simoni D, Rizzi M, Rondanin R, Baruchello R, Marchetti P, Invidiata FP, Labbozzetta M, Poma P, Carina V, Notarbartolo M, Alaimo A, D'Alessandro N. Antitumor effects of curcumin and structurally beta-diketone modified analogs on multidrug resistant cancer cells. *Bioorg Med Chem Lett.* 2008;18:845-849.
32. Suo A, Qian J, Xu M, Xu W, Zhang Y, Yao Y. Folate-decorated PEGylated triblock copolymer as a pH/reduction dual-responsive nanovehicle for targeted intracellular co-delivery of doxorubicin and Bcl-2 siRNA. *Mater Sci Eng C Mater Biol Appl.* 2017;76:659-672.
33. Suo A, Qian J, Zhang Y, Liu R, Xu W, Wang H. Comb-like amphiphilic polypeptide-based copolymer nanomicelles for co-delivery of doxorubicin and P-gp siRNA into MCF-7 cells. *Mater Sci Eng C Mater Biol Appl.* 2016;62:564-573.
34. Wu J, Zhang J, Jiang M, Zhang T, Wang Y, Wang Z, Miao Y, Wang Z, Li W. Comparison between NOD/SCID mice and BALB/c mice for patient-derived tumor xenografts model of non-small-cell lung cancer. *Cancer Manag Res.* 2018;10:6695-6703.
35. Xiao CQ, Chen R, Lin J, Wang G, Chen Y, Tan ZR, Zhou HH. Effect of genistein on the activities of cytochrome P450 3A and P-glycoprotein in Chinese healthy participants. *Xenobiotica.* 2012;42:173-178.
36. Yuan J, Yin Z, Tan L, Zhu W, Tao K, Wang G, Shi W, Gao J. Interferon regulatory factor-1 reverses chemoresistance by downregulating the expression of P-glycoprotein in gastric cancer. *Cancer Lett.* 2019;457:28-39.
37. Zhang J, Chen Y, Li X, Liang X, Luo X. The influence of different long-circulating materials on the pharmacokinetics of liposomal vincristine sulfate. *Int J Nanomedicine.* 2016;11:4187-4197.
38. Zhang W, Liu M, Yang L, Huang F, Lan Y, Li H, Wu H, Zhang B, Shi H, Wu X. P-glycoprotein inhibitor tariquidar potentiates efficacy of astragaloside IV in experimental autoimmune encephalomyelitis mice. *Molecules.* 2019;24:561.
39. Zhang S, Yang X, Morris ME. Combined effects of multiple flavonoids on breast cancer resistance protein (ABCG2)-mediated transport. *Pharm Res.* 2004;21:1263-1273.
40. Yue Q, Xu Y, Deng X, Wang S, Qiu J, Qian B, Zhang Y. Circ-PITX1 promotes the progression of non-small cell lung cancer through regulating the miR-1248/CCND2 axis. *Onco Targets Ther.* 2021;14:1807-1819.
41. Lee ACK, Lau PM, Kwan YW, Kong SK. Mitochondrial fuel dependence on glutamine drives chemo-resistance in the cancer stem cells of hepatocellular carcinoma. *Int J Mol Sci.* 2021;22:3315.
42. Zhao BX, Sun YB, Wang SQ, Duan L, Huo QL, Ren F, Li GF. Grape seed procyanidin reversal of p-glycoprotein associated multi-drug resistance via down-regulation of NF-κB and MAPK/ERK mediated YB-1 activity in A2780/T cells. *PLoS One.* 2013;8:e71071.